Analysis of Part Accessibility in Product Disassembly

Qingjin Peng and Chulho Chung

University of Manitoba, Pengq@cc.umanitoba.ca, umchung9@cc.umanitoba.ca

ABSTRACT

This paper introduces a novel approach to the analysis of parts' geometric accessibility for product disassembly. Given solid models of a product consisting of parts and fasteners, the goal is to quickly determine whether a part in the product is accessible or not. A feasible disassembly plan can then be decided based on the constraints of a given part configuration and the fastener type. The system developed using the proposed method can simulate a part disassembly process in a computer generated 3D environment. The simulation can clearly verify whether the process is appropriate or not for a fastener disassembling.

Keywords: disassembly, accessibility, product design.

1. INTRODUCTION

Disassembly planning defines the sequence of a product disassembly, by which an initially completed product is separated into individual parts for repair or recycle. A feasible plan results in less fixturing, less tooling, and more reliable operations in the disassembly of a product. An improper product disassembly plan may lead to special tooling, or design changing for the product maintenance. Therefore, the disassembly planning is a crucial process in the product life-cycle [1].

A key factor in disassembly planning is the available space for the disassembly of a part. Comparing with other methods developed for product assembly or disassembly plan, the analysis of parts accessibility in disassembly within the available space is a relatively under-explored issue, especially for the selected disassembly to disassemble only selected parts in a product for the parts replacement. Some existing methods are computationally expensive to implement. Current analysis of product disassembly related to the operation space is mainly executed via physical simulation, virtual simulation, or interactive user-knowledge. These approaches are not efficient in dealing with various what-if scenarios of product disassembly. These methods also tend to depend on users' expertise or experience.

Disassemblability of a product is a function of several parameters such as exertion of manual force for disassembly, degree of precision required for effective tool placement, weight, size, material and shape of components being disassembled, and use of hand tools [2]. Topological disassemblability is based on the geometric constraints that the shape of parts creates in a product. In non-destructive disassembly planning, the topological disassemblability determines the priority of parts being disassembled. With the disassembly-tool feasibility, this constraint forms a means to generate a practical and realistic plan for disassembly.

This research analyses the geometric accessibility of parts disassembly. Given solid models of a product consisting of parts and fasteners, the goal is to quickly determine whether the part in a disassembly is accessible or not. A feasible disassembly plan is then decided based on the constraints of a given part configuration, the fastener type and tool availability. The system developed will simulate the disassembly in a computer generated 3D environment. The simulation can clearly verify whether the process is appropriate or not in a fastener disassembling.

2. RELATED RESEARCH

Disassembly planning plays a key role in de-manufacturing (DM). It aims to generate a disassembly sequence with subsequent disassembly actions [3]. The initial attempt of disassembly planning was rooted in assembly planning. Using the various methods developed for assembly planning, a disassembly sequence is determined by the separation of an assembly into two or more subassemblies. It is called reverse assembly planning, which is based on the complete reverse assembly or disassembly analysis of a product. However, disassembly is usually not performed to its full extent,

and incomplete disassembly is often preferred for DM. Although a partial disassembly for DM can be obtained from a complete disassembly analysis, it does not guarantee an optimal disassembly sequence for DM.

Selected disassembly (SD) is partial and incomplete disassembly of a product. SD is defined as the disassembly of selected parts in a product. The SD aims to minimize efforts to separate parts selected for separation or replacement. The SD by unscrewing fasteners is often required for such activities as maintenance or repair, product reuse, product recycling or remanufacturing. Without damaging components, non-destructive SD aims to quickly isolate selected parts, not including any part of joining elements-fasteners. This enables resources, such as materials and energy, used for a product in manufacturing to be preserved. Thus, this method has the highest priority from the environmental point of view [4.5].

Component-based sequence planning for SD has been addressed by several researchers. As a major approach to SD sequence planning, the wave propagation (WP) method was suggested by Srinivasan and Gadh [6]. This method defines disassembly waves to topologically arrange the parts associated with the disassembly of selected parts. It plans an optimal disassembly sequence based on the waves. The WP method uses two objectives in reducing the SD cost, minimizing the number of component removals and the total weight of components to disassemble [7].

Garcia *et al*. [8] proposed an approach to reduce the computational complexity of the WP method. Instead of constructing waves for selected parts, the approach searches for an optimal disassembly sequence via a predefined precedence graph that describes the shortest path to all exterior nodes. Another effort to reduce the complexity was made by Mascle and Balasoiu [9]. The authors suggested an algorithmic approach to choose a minimal number of parts that form disassembly waves based on the WP method. However, these approaches based on topological disassemblability of parts ignore two important issues: batch disassembly of parts for minimizing efforts in SD, and the parts accessibility in partial and non-sequential disassembly.

A potential approach to SD integrating batch disassembly of parts and the parts accessibility to fasteners can be developed from the fastener-based approaches used in assembly or disassembly sequence planning. Akagi *et al*. [10] initially emphasized the significance of fasteners in assembly sequence planning. Gui and Mantyla [11] used fasteners as a description of features to provide constraints for joint components. However, these investigations only focused on assembly modeling based on the nature of fasteners. In Kuo's research [12], a method was proposed to decompose an assembly into subassemblies connected by fasteners. It starts with identifying cut-vertices, bi-connected graph and pendent vertices in a component-fastener graph via the depth first search (DFS) algorithm. Disassembly sequence is planned using an objective function and the disassembly precedence matrix based on the identified subassemblies. Tseng and Li [13] decomposed an assembly into a set of fastener-based subassemblies, and then generated assembly sequences by an interference-checking method based on CAD boundary representation (B-rep). Furthermore, Yin *et al*. [14] decomposed an assembly into a set of fastener-based subassemblies with hierarchical structure. They used a relational model graph [15] instead of the CAD B-rep interference checking [13]. However, these approaches fail to notice the importance of the part accessibility because they mainly focus on the generation of a complete procedural assembly or disassembly sequence for a product with fastener-based structure. Although an SD sequence for selected parts may be obtained from a complete disassembly analysis by the above approaches, there is no guarantee that this will generate an efficient and optimal sequence for SD.

This research develops an approach to topological disassemblability analysis of parts. The part disassemblability analysis works based on two matrices: the fastener-part connectivity matrix and the part accessibility matrix. A systematic method is also presented to construct these matrices from a CAD file. A digitized assembly directionality chart is proposed to simply the analysis.

3. THE BASIS OF PART ACCESSIBILITY IN PRODUCT DISASSEMBLY

3.1 The Relation of Fasteners, Parts, and the Part Disassembly Directionality

The relation between fasteners and parts, and the part disassembly directionality can be expressed by two matrices. The matrix *FP* that represents connectivity between fasteners and parts is defined in Equation (1). The row and column vectors represent the fastener and part sets, *M* and *N*, in a product, respectively. In Equation (1), $FP_{i,j}$ is 1 if fastener *i* is connected to part *j* otherwise, 0.

$$\mathbf{FP} = \begin{array}{c} \\ 1 \\ 2 \\ \vdots \\ i \end{array} \begin{array}{c} \begin{array}{cccc} 1 & 2 & \cdots & j \end{array} \\ \begin{bmatrix} FP_{1,1} & FP_{1,2} & \cdots & FP_{1,j} \\ FP_{2,1} & FP_{2,2} & \cdots & FP_{2,j} \\ \vdots & \vdots & \ddots & \vdots \\ FP_{i,1} & FP_{i,2} & \cdots & FP_{i,j} \end{bmatrix} \end{array} \quad (i = 1, 2, \cdots, m;\ j = 1, 2, \cdots, n) \tag{1}$$

$$\text{Where, } FP_{i,j} = \begin{cases} 1 & \text{if fastener } i \text{ is connected to part } j \\ 0 & \text{otherwise} \end{cases}$$

Accessibility of part *i* to its adjacent part *j* is defined as the set of directions with which part *i* can be moved relative to part *j*, and is denoted as a directionality matrix, $\boldsymbol{PA}^{i,j}$ [7]. Equation (2) shows the matrix $\boldsymbol{PA}$.

$$\mathbf{PA} = \begin{array}{c} \\ 1 \\ 2 \\ \vdots \\ i \end{array} \begin{array}{c} \begin{array}{cccc} 1 & 2 & \cdots & j \end{array} \\ \begin{bmatrix} \mathbf{PA}^{1,1} & \mathbf{PA}^{1,2} & \cdots & \mathbf{PA}^{1,j} \\ \mathbf{PA}^{2,1} & \mathbf{PA}^{2,2} & \cdots & \mathbf{PA}^{2,j} \\ \vdots & \vdots & \ddots & \vdots \\ \mathbf{PA}^{i,1} & \mathbf{PA}^{i,2} & \cdots & \mathbf{PA}^{i,j} \end{bmatrix} \end{array} \quad (i, j = 1, 2, \cdots, n) \tag{2}$$

A directionality matrix $\boldsymbol{PA}^{i,j}$ in Equation (2) consists of a set of directions. Corresponding to the matrix size of $\boldsymbol{PA}^{i,j}$, the number of directions can be increased by a user definition in a coordinate system. For instance, Fig. 1(a) shows 6 directions, ±*x*, ±*y* and ±*z*, defined in the Cartesian coordinate system.

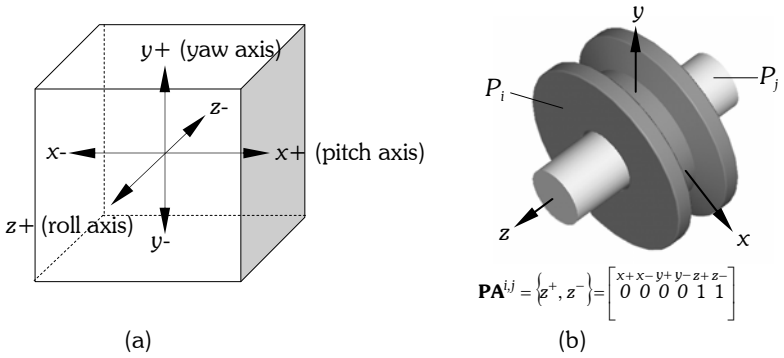

Fig. 1: An example of defining an element $\boldsymbol{PA}^{i,j}$: (a) 6 directions in the Cartesian coordinate system, and (b) representation of the element $\boldsymbol{PA}^{i,j}$.

Part *i* shown in Fig. 1(b) can only move relative to part *j* along the two directions, *z*+ and *z*-. Thus, the element $\boldsymbol{PA}^{i,j}$ is represented as [*x*+:*x*-:*y*+:*y*-:*z*+:*z*-⇒*000011*], where *0* and *1* respectively represent an inaccessible direction, and an accessible direction. Similarly, if part *i* equals to part *j*, the element $\boldsymbol{PA}^{i,i}$ in the matrix $\boldsymbol{PA}$ has the complete set of six-directions, ±x, ±y and ±z, and is represented as [111111]. For a part Pi, topological disassemblability (Δi) within the set N can be determined by following Equation (3).

$$\Delta i = \begin{cases} 1 & \text{if} \bigcap_{j \in \mathbf{N}} \mathbf{PA}^{i,j} \neq \Phi, \text{ subject to } \sum_{k} FP_{k,i} = 0,\ k \in \mathbf{M} \\ 0 & \text{otherwise} \end{cases} \tag{3}$$

Equation (3) represents that a part satisfying these geometric constraints should not be connected with any fastener when it is disassembled. The fastener constraint in Equation (3) is generally satisfied by the two following cases: (1) there is no fastener connecting the part, and (2) all related fasteners are removed before disassembling the part.

3.2 Primitive Matrices

A systematic method is used to automatically construct the primitive matrices **FP** and **PA** from a CAD file represented in VRML (virtual reality modelling language). A component in this research is referred to as a set of triangle patches, which is widely used for solid representations in computer graphics. Fig. 2 shows the hierarchical structure of a product CAD model used in this research.

As shown in Fig. 2, a product consists of a number of parts and fasteners. The product is normally generated from an assembly CAD model integrating part and fastener CAD models via a CAD system. Each component like a part or a fastener is represented as a number of triangle patches, each patch is defined by three vertices $\boldsymbol{V}_0^i$, $\boldsymbol{V}_1^i$ and $\boldsymbol{V}_2^i$, and its normal vector $\boldsymbol{n}_i$.

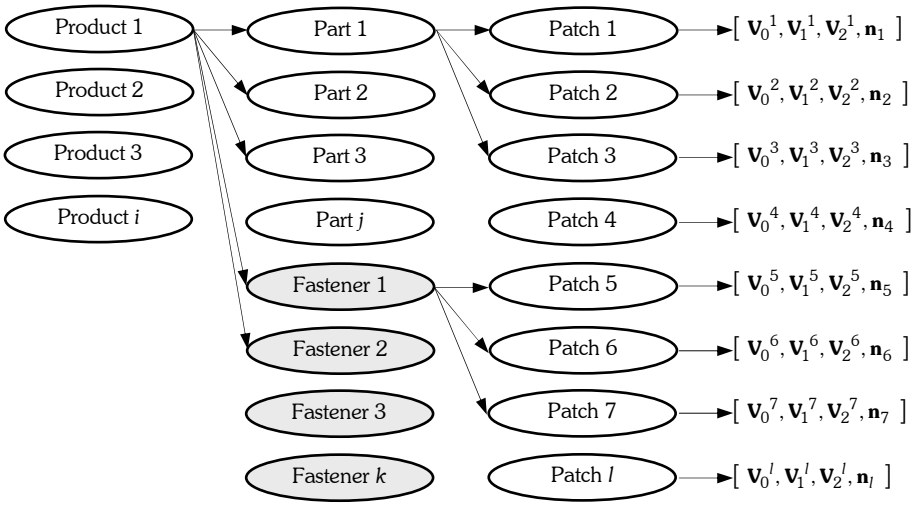

Fig. 2: Hierarchical structure of a product CAD model used in this research.

For determining primitive matrices ***FP*** and ***PA***, several collision detection methods based on triangle patches are used in this research. A collision between components is quickly detected by the algorithm developed, which combines bounding sphere- (BS), oriented bounding box- (OBB), and triangle patch-based methods.

Algorithm 1 describes the procedure to determine fastener interference in constructing the matrix ***FP***. This algorithm can quickly find the triangle patch of a part, which might collide with a fastener. It starts with the BS-based test with two bounding spheres, BS_i and BS_j approximating fastener i (*i.e.*, F_i, $i \in \boldsymbol{M}$) and part j (*i.e.*, P_j, $j \in \boldsymbol{N}$), respectively. If a collision is detected between BS_i and BS_j, the F_i and P_j are respectively approximated into oriented bounding boxes OBB_i and OBB^j for a more precise collision test. The OBB^j is divided in two OBBs via the top-down approach in the hierarchical OBB-tree method [16] if a collision still exists between OBB_i and OBB^j. Two oriented bounding boxes, $OBB^j{}_1$ and $OBB^j{}_2$ are again applied to the OBB-based test to choose a new OBB^j with collision. This division process is continuously executed while a collision with the OBB_i occurs in either $OBB^j{}_1$ or $OBB^j{}_2$, and a chosen oriented bounding box with the collision consists of two or more triangle patches.

As shown in Algorithm 1, subsequently, the triangle-triangle intersection test is carried out via one triangle patch of the OBB_i and the interfered patch k (*i.e.*, T_k^j in Algorithm 1) of P_j. Moreover, a binary value (*i.e.*, *0* or *1*) for an element $FP_{i,j}$ in the matrix ***FP*** is determined by the result of this test. Fig. 3 shows the overall procedure of determining fastener interference via Algorithm 1.

Algorithm 1: Determination of the matrix ***FP***

Input part and fastener sets, **N** and **M**
For $i = 1, \ldots, m \Rightarrow$
  Generate BS_i based on fastener F_i
  For $j = 1, \ldots, n \Rightarrow$
    Let $FP_{i,j} = 0$
    Generate BS_j based on part P_j
    Execute BS-based collision test (BS_i, BS_j)
    If there is a collision then
      Generate OBB_i based on fastener F_i
      Generate OBB^j based on part P_j
      Execute the OBB-based collision test (OBB_i, OBB^j)
      Do while (there is a collision) $\Rightarrow$
        If OBB^j is defined by only a triangle patch ${T_k}^j$ then
          Take a triangle patch (T_i) from OBB_i
          Execute triangle-to-triangle interference test $(T_i, {T_k}^j)$
          If there is a collision then $FP_{i,j} = 1$
          Exit Do
        Else
          Partitioning OBB^j via the hierarchical OBB-tree method $\Rightarrow$
          ${OBB^j}_1$ and ${OBB^j}_2$
          Execute the OBB-based collision test $(OBB_i, {OBB^j}_1)$
          Execute the OBB-based collision test $(OBB_i, {OBB^j}_2)$
          Let $OBB^j = {OBB^j}_1$ or ${OBB^j}_2$ if there is a collision

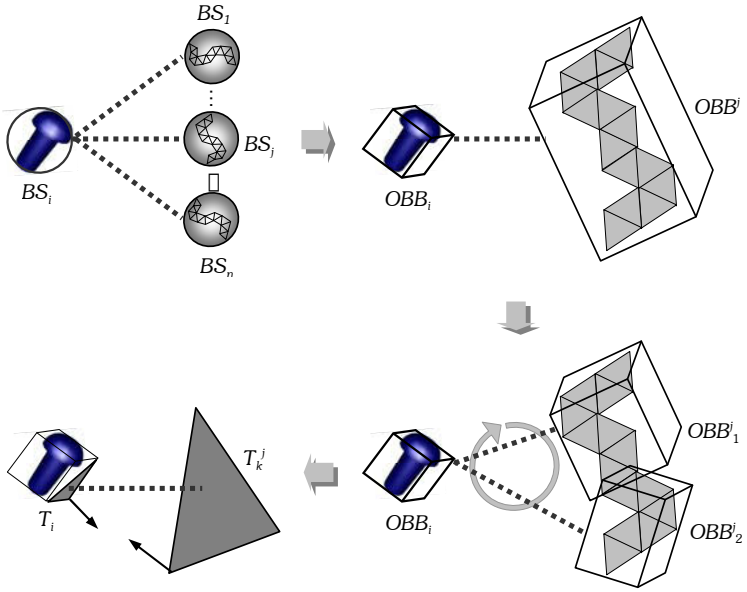

Fig. 3: Overall procedure of determining fastener interference via Algorithm 1.

Determining $\boldsymbol{PA}^{i,j}$ ($i \neq j$ and $i,j \in \boldsymbol{N}$) in the matrix $\boldsymbol{PA}$ is a computationally intensive process because all disassembly directions should be considered for all part combinations that have complex shapes with a large number of triangle patches. Therefore, a digitized disassembly directionality chart (D^3C) is introduced.

4. A DIGITIZED ASSEMBLY DIRECTIONALITY CHART

Based on the concept of discrete global accessibility cones [17, 18], a digitized assembly directionality chart (D^3C) is proposed in this research, which is shown in Fig. 4. The D^3C is formed to store direction information for determining part accessibility. A D^3C represents approximate surroundings around a part to be disassembled. The surroundings are based on the geometric configuration of parts in a product. The D^3C consists of 180×360 pixels to make a total of 64,800 directions on a discrete unit sphere. The number of pixels is exactly matched with 180 colatitude angles (φ) and 360 longitude angles (θ) in the Spherical coordinate system. The pixels of a D^3C are simply represented as the Boolean data type, *true* (inaccessible) or *false* (accessible), which is used for searching accessible directions of a part. Therefore, there is a one-to-one mapping between directions in the D^3C and unit vectors in the Spherical coordinate system. Thus, φ and θ in this research are used to calculate a unit vector and to indicate the direction at an equivalent pixel (θ,φ). In the Spherical coordinate system, a unit vector based on a pixel (θ,φ) is simply determined as follows.

$$\hat{\mathbf{T}}(\theta,\varphi) = (\sin\varphi \sin\theta)\hat{\mathbf{i}} + (\cos\varphi)\hat{\mathbf{j}} + (\sin\varphi \cos\theta)\hat{\mathbf{k}} \tag{4}$$

To efficiently generate a D^3C for the accessibility of part i to its adjacent part j, two mapping processes are presented, which are only based on two bounding spheres (BSs) with no collision and two triangle patches with collision. A bounding sphere is approximately obtained from not only a part with no collision, but also an oriented bounding box (OBB) with no collision during the repeating process of the OBB division and collision detection.

During the process, therefore, one or more sets of bounding spheres are generated for two parts, P_i ($i \in \boldsymbol{N}$) and P_j ($j \in \boldsymbol{N}$), and these sets are mapped into the D^3C. If P_i and P_j are contacted, two triangle patches with collision are subsequently detected, and mapped into the D^3C via the triangle patch-based mapping process. This is the worst case, and computationally expensive because the collision detection tests are continuously executed from the top level to the bottom level of two parts. Both bounding sphere-based mapping processes and a triangle patch-based mapping process are subsequently executed for this case. Fig. 5 shows two mapping processes: bounding sphere- and triangle patch-based mapping processes.

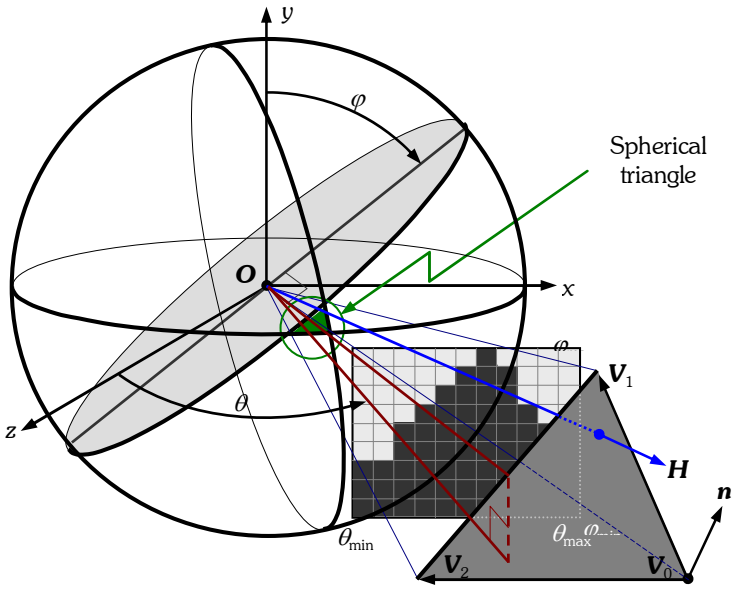

Fig. 4: Construction of a D^3C.

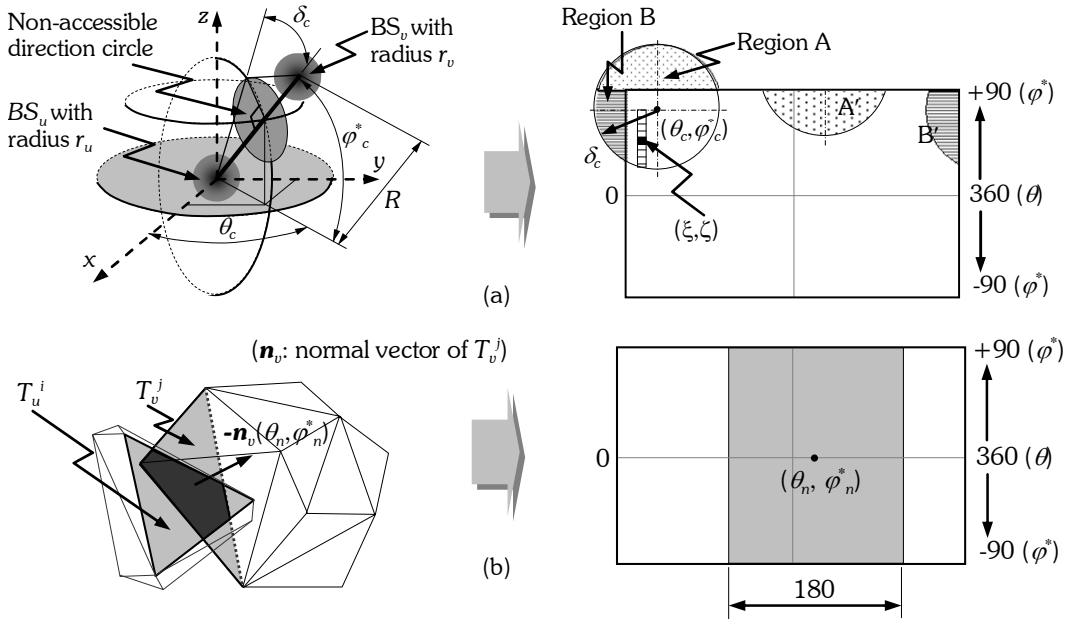

Fig. 5: Determination of the D^{3}C for part accessibility: (a) mapping to a D^{3}C with non-accessible direction circle between two bounding spheres, and (b) mapping to a D^{3}C with two contacting patches.

In Fig. 5(a), a non-accessible direction circle is defined if there is no collision between given two bounding spheres, BS_u and BS_v. The BS_u or BS_v is approximately obtained from not only a part with no collision, but also an oriented bounding box with no collision during the repeating process of the bounding box division and collision detection. The non-accessible direction circle in Fig. 5(a) is a blocking region consisting of a set of directions between two bounding spheres, and is represented by longitude (θ), latitude (φ^*) and radius (δ). If a vector between BS_u and BS_v in Fig. 5(a) is represented by $x\hat{\mathbf{i}} + y\hat{\mathbf{j}} + z\hat{\mathbf{k}}$, the non-accessible direction circle is defined by Equation (5).

$$\begin{cases} \varphi^*_C = \sin^{-1}(z/R) \\ \theta_C = \tan^{-1}(y/x) \\ \delta_C = \sin^{-1}\{(r_u + r_v)/R\} \end{cases} \tag{5}$$

Where, $R = \left[x^2 + y^2 + z^2\right]^{1/2}$. As shown in Fig. 5(a), subsequently, a defined non-accessible direction circle by Equation (5) is mapped into the D^{3}C for a part accessibility.

As shown in Fig. 5(b), a part P_i is in contact with another part P_j, and two touching triangle patches are T_u^i and T_v^j. In this case, a non-accessible direction region of 180×180 degree is mapped into the D^{3}C shown in Fig. 5(b). The centre point of this square region is the negative normal vector $-\mathbf{n}_v\left(\theta_n, \varphi^*_n\right)$ of T_v^j. Similar to the result from Gaussian sphere-based approaches [19, 20], the square region results in blocking half of the disassembly directionality space for the disassembly of part *i*.

In particular, to fit all the angles ξ and ζ digitized from non-accessible direction shapes into a D^{3}C, this research uses several transformation equations, one of which is introduced as follows.

$$If\ |\zeta| > 90^{\circ} \begin{cases} \xi = [360 + (180 + \xi)] \bmod 360 \\ \zeta = \zeta / |\zeta| (180 - |\zeta|) \end{cases} \quad (6)$$

This equation is applied for both mapping processes shown in Figs 5(a) and (b). By Equation (6), for instance, region *A* shown in Fig. 5(a) is transformed to regions *A'*. Subsequently, all the transformed angles ξ and ζ are fitted into the D^3C for a part accessibility.

5. EXAMPLES

As shown in Figs. 6 and 7, a product is selected to test the proposed method. The product consists of 17 parts and 20 fasteners including bolts, screws and nuts. The same types of the fasteners are used in this product, which are 1/4″ hex type fasteners.

Fig. 6 shows the test for part P_1 disassembleability relative to part P_6. The white region of the D^3C in Fig. 6 represents an available disassembly directionality region for P_1 while the rest of the regions represent non-accessible directions. In particular, the available disassembly directionality region is a set of accessible directions; each direction allows the disassembling of P_1 relative to P_6. This set of accessible directions is converted to the direction cone shown in Fig. 6.

Several other parts of the product are tested as shown in Fig. 7. Grey coloured regions in Fig. 7 are formed by non-accessible direction circles or regions, both of which are defined by the mapping processes shown in Fig. 4. In particular, Figs 7(b) and (c) illustrate the disassemblability tests for two contacted parts. In Fig. 7(b), for instance, a non-accessible direction region of 180×180 degree is mapped into the D^3C of the parts P_1 and P_5 after automatically detecting two-contacted triangle patches of P_1 and P_5. The centre point of this square is defined by $-\mathbf{n}_v(\theta_n, \varphi^*_n)$, the (-) normal vector of the contacted patch of P_5. This is the same result of the Gaussian sphere-based approaches [19, 20], resulting in blocking half of the disassembly directionality space for the disassembly of P_1.

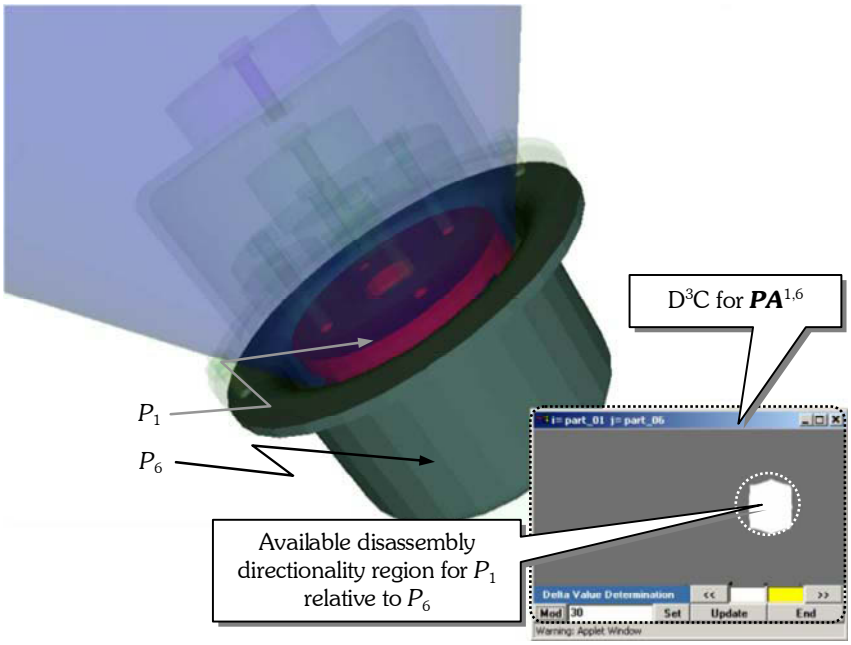

Fig. 6: Part P_1 disassembleability relative to part P_6

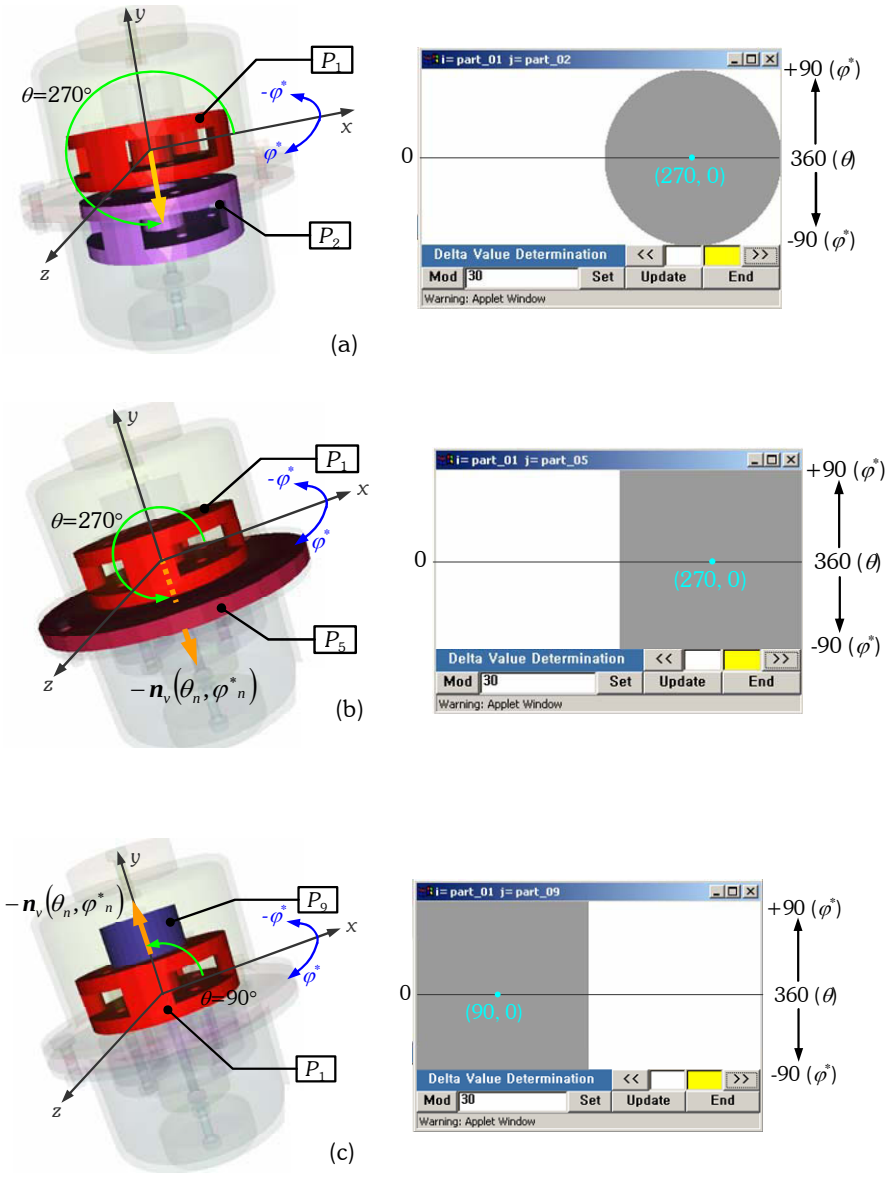

Fig. 7: Test results of parts accessibility (a) Parts 1 & 2, (b) Parts 1 & 5 and (c) Parts 1 & 9.

6. CONCLUSIONS AND FURTHER WORK

This paper presented an approach to topological disassemblability analysis of parts in a product. A systematic method is developed to construct two primitive matrices from a CAD file. Several collision detection methods are used in this research, namely BS-, OBB-, and triangle patch-based collision detection methods. A digitized disassembly directionality chart, a D^3C, is introduced to represent the part accessibility. In determining complicated topological disassemblability, the D^3C allows for mapping 3D geometric constraints between parts into a 2D directionality map. This is advantageous for searching available directions for a part assembly or disassembly.

The further work is to introduce human factor into an assembly or disassembly planning. Human-involved planning covers not only the generation of realistic, economical and optimal plans, but also the analysis of potential risks occurring by people during the operations.

7. ACKNOWLEDGEMENTS

This research is supported by Canadian NSERC Discovery Grants, and the University of Manitoba Graduate Fellowships.

8. REFERENCES

[1] Noh, D. S.; Park, J. Y.; Kong, H. S.; Han, G. Y.; Kim, G.; Lee, I. K.: Concurrent and collaborative process planning for automotive general assembly, International Journal of Advanced Manufacturing Technology, DOI: 10.1007/S00170-004-2092-9, 2004.

[2] Desai, A.; Mital, A.: Evaluation of disassemblability to enable design for disassembly in mass production, International Journal of Industrial Ergonomics, 32, 2003, 265–281.

[3] Lambert, A. J. D.: Disassembly sequencing: a survey, International Journal of Production Research. 41(16), 2003, 3721-3759.

[4] Bras, B.: Design for Recycling, www.srl.gatech.edu/education/ME4171/DFR-Intro.ppt, 2004.

[5] Shu, H. L.; Flowers, C. W.: Application of a design-for-remanufacture framework to the selection of product life-cycle fastening and joining methods, Robotics and Computer Integrated Manufacturing, 15, 1999, 179-190.

[6] Srinivasan, H.; Gadh, R.: A geometric algorithm for single selective disassembly using the wave propagation abstraction, Computer Aided Design, 30, 1998, 603-613.

[7] Srinivasan, H.; Figueroa, R.; Gadh, R.: Selective disassembly for virtual prototyping as applied to de-manufacturing, Robotics and Computer-Integrated Manufacturing, 15, 1999, 231-245.

[8] Garcia, M. A.; Larre, A.; Lopez, B.; Oller, A.: Reducing the complexity of geometric selective disassembly, Proceedings of IEEE/RSJ International Conference on Intelligent Robots and Systems, 2000, 1474-1479.

[9] Mascle, C.; Balasoiu, B.: Algorithmic selection of a disassembly sequence of a component by a wave propagation method, Robotics and Computer-Integrated Manufacturing, 19, 2003, 439-448.

[10] Akagi, F.; Osaki, H.; Kikuchi, S.: The method of analysis of assembly work based on the fastener method, Bulletin of the JSME, 23, 1980, 1670-1675.

[11] Gui, J. K.; Mantyla, M.: Functional understanding of assembly modeling, Computer Aided Design, 26(6), 1994, 435-451.

[12] Kuo, C. T.: Disassembly sequence and cost analysis for electromechanical products, Robotics and Computer-Integrated Manufacturing, 16, 2000, 43-54.

[13] Tseng, E. H.; Li, K. R.: A novel means of generating assembly sequences using the connector concept, Journal of Intelligent Manufacturing, 10, 1999, 423-435.

[14] Yin, P. Z.; Ding, H.; Li, X. H.; Xiong, L. Y.: A connector-based hierarchical approach to assembly sequence planning for mechanical assemblies, Computer Aided Design, 35, 2003, 37-56.

[15] Homem De Mello, S. L.; Sanderson, C. A.: A correct and complete algorithm for the generation of mechanical assembly sequences, IEEE Transactions on Robotics and Automation, 7, 1991, 228-240.

[16] Gottschalk, S.; Lin, M. C.; Manocha, D.: OBB-Tree: A hierarchical structure for rapid interference detection, Proceedings of the 23rd Annual Conference on Computer Graphics and Interactive Techniques, New York, 1996, 171-180.

[17] Spitz, N. S.; Spyridi, J. A.; Requicha, A. G. A.: Accessibility analysis for planning of dimensional inspection with coordinate measuring machines, IEEE Transactions on Robotics and Automation, 15(6), 1999, 714-727.

[18] Spitz, N. S.; Requicha, A. G. A.: Accessibility analysis using computer graphics hardware, IEEE Transactions on Visualization and Computer Graphics, 6(3), 2000, 208-219.

[19] Mo, J.; Zhang, Q.; Gadh, R.: Virtual disassembly, International Journal of CAD/CAM, 2(1), 2002, 29-37.

[20] Pomares, J.; Puente, S. T.; Torres, F.; Candelas, F. A.; Gil, P.: Virtual disassembly of products based on geometric models, Computers in Industry, 55, 2004, 1-14.